

A COMPARISON OF D-AXIS STATOR CURRENT CONTROL METHODS FOR TWO PMSG PARALLEL - OPERATED BASED ON WIND TURBINE SYSTEMS

NGUYEN NGOC ANH TUAN ^{1*}, DUY CONG PHAM ¹, NGUYEN THANH THAO ¹,
VO THI ANH TUYET ¹, BUI HONG PHONG ²

¹ Faculty of Electrical Engineering, Industrial University of Ho Chi Minh City, Vietnam,

² Nguyen Huu Canh Technical and Economic College, Ho Chi Minh City, Vietnam;

*Corresponding author: nguyenngocanhluan@iuh.edu.vn

DOIs: <https://doi.org/10.46242/jstiuh.v70i4.4854>

Abstract. This paper proposes a study of d-axis stator current control technique for machine side converter in the permanent magnet synchronous generator based on two parallel-operated wind turbine systems which is connected to the grid via back- to-back converters. A reviewed shortly of d-axis stators current control techniques are presented. The zero d-axis stator current (ZDC) control technique is firstly, the second control is the unity power factor (UPF) control technique and the third is the constant stator flux-linkage (CSF) control technique. Comparative studies are presented to validate the advantageous features of the proposed methods. The performance of the proposed is assessed and compared through a simulation results based on MATLAB. The comparative results show that the superiority of the proposed methods are proved by the d-axis stator current control can not only attended well the maximum power but also can be reduced costly.

Keywords. Permanent Magnet Synchronous Generator, zero direct axis stator current control, unity power factor control, constant stator mutual flux linkages control.

1 INTRODUCTION

Wind Turbine systems have received a great deal of attention in the last decade as one of the most promising renewable energy sources, owing to the potential depletion, high prices, and negative environmental implications of traditional energy sources [1]. Wind energy is a non-polluting and limitless resource. As a result, a wind energy producing system might be one of the future's possible sources of alternative energy [2,3].

Wind energy conversion system that consists of a generator, a back-to-back converter, a filter and a transformer [2]. According to [1], PMSG generators have the main advantages over other types because of their high efficiency and the elimination of the slip rings, a simpler gearbox, and full power controllability during the grid faults, saving costs and maintenance time [4]. The wind turbine configuration, which is based on the PMSG, employs a full-scale power converter and it is shown in Fig.1. The generator stator winding is connected to the grid through the full-scale power converter, which performs the reactive power compensation and a smooth grid connection for the entire speed range of the generator. The power converter can be divided into the machine side converter and the grid side converter due to their positions [5,6]. The WECS control is becoming increasingly important, especially when using the PMSG-based electrical generator. In [7] presented the mathematical model, dynamic response assessment and controller of the system. Multi-scale transients modeling and simulation for PMSG-based wind power systems is presented in [8]. However, the disadvantages lie in the design modeling, characteristics of stator- and rotor resistance, inductance and complex.

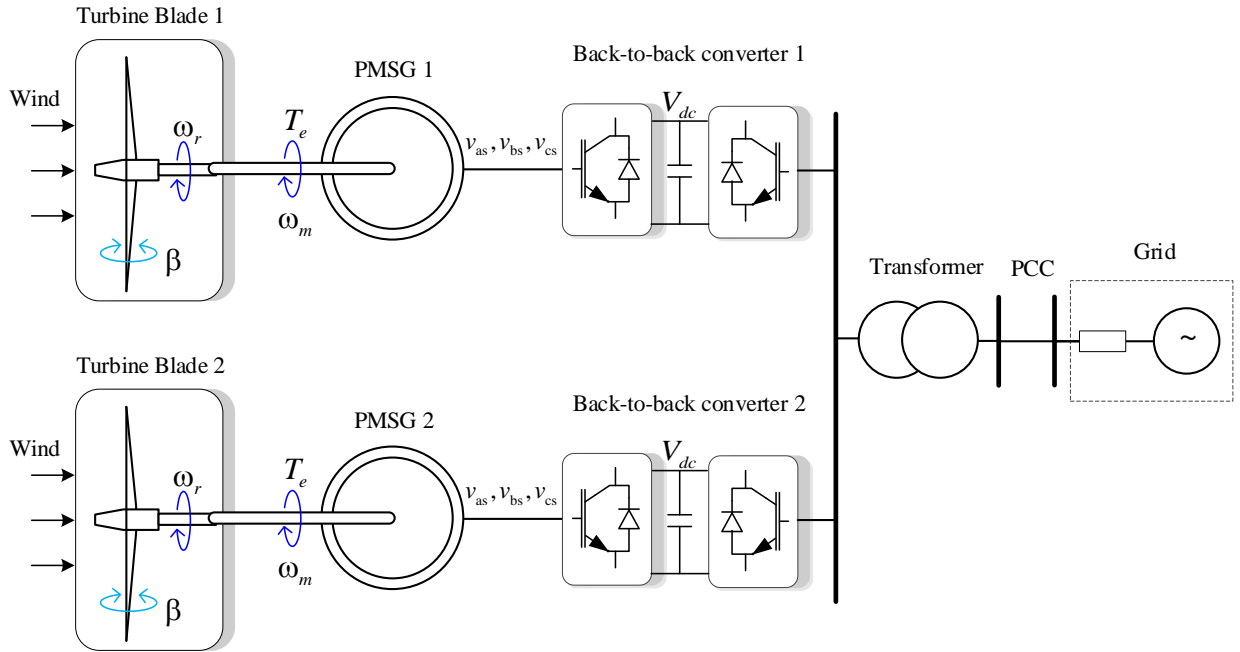


Figure 1: The overall structure of PMSG wind energy system

In [9] introduced three control methods, included the direct-axis component of the stator current is set to zero (ZDC), the power factor being kept equal to one (UPF), and constant stator flux-linkages (CSF), that were used to apply for the PMSM. In the industry, the direct-axis component of the stator current is set to zero that is frequently employed. Its own advantages are that it is simple to use and that it has a low power factor. The main disadvantage of the UPF control is that it produces a low-torque per unit current ratio while optimizing the system's perceived power (volt-ampere consumption) through the maintenance of the power factor at unity. The air gap flux linkages are restricted by the CSF control mechanism to any predetermined or desired flux linkages. It should be noted that this control has yet applied for PMSG. The direct-axis component of the stator current is set to zero and the power factor is kept equal to one, that is compared to create an optimal control for the machine side converter of the Z-source [10]. To determine the highest power point for the machine side converter, the hysteresis controller is paired with the ZDC control [11], but this involves extensive calculation and algorithm modeling. The purpose of this study is to present three direct-axis currents control strategies for machine side converter of PMSG. The main contribution of this paper can be outlined as follows.

- A comparative study of the three d-axis stator current control methods for two PMSG parallel - operated based on wind turbine systems.
- ZDC, UPF and CSF control methods are successful applied for two PMSG parallel - operated based on wind turbine systems. Their performance is assessed and compared using key characteristics such as generator power coefficient and grid power coefficient under the same operating conditions.
- Based on the control theory of permanent magnet synchronous machines (PMSM), the control theory for two PMSGs operating in parallel in a wind turbine system can be developed.

2 MODELING OF WIND TURBINE SYSTEMS

2.1 Wind turbine model

Wind turbine has the mainly function of converting mechanical energy, formed to extract kinetic energy from different wind speed with rotor mechanical velocity, into electrical energy. The mechanical output power of the turbine is given by the following equation.

$$P_m = \frac{1}{2} \rho \pi R^2 C_p(\alpha, \beta) v_{wind}^3 = K_p C_p(\alpha, \beta) v_{wind}^3 \quad (1)$$

where P_m is mechanical power (W), ρ is the density of air for turbine (kg/m^3), R is the blade length (m), v_{wind} is the wind speed (m/s), C_p is the power coefficient, α is tip speed ratio, β is pitch angle of blade (deg). The tip speed ratio and power coefficient can be calculated as follows.

$$\alpha = \frac{\omega_m R}{v_{\text{wind}}} \quad (2)$$

where ω_m represent the turbine rotor radius (rad/s).

$$C_p(\alpha) = c_1 \left(\frac{c_2}{\alpha_i} - c_3 \beta - c_4 \right) e^{\left(\frac{-c_5}{\alpha_i} \right)} + c_6 \alpha \quad (3)$$

where wind turbine coefficients c_1 to c_6 are: $c_1 = 0.5176$; $c_2 = 116$; $c_3 = 0.4$; $c_4 = 5$; $c_5 = 21$; $c_6 = 0.0068$;

2.2 PMSG model

The stator voltage u_{ds} and u_{qs} expressed in the dq reference frame can be clarified as below.

$$u_{ds} = R_s i_{ds} + L_d \frac{di_{ds}}{dt} - \omega_r L_q i_{qs} \quad (4)$$

$$u_{qs} = R_s i_{qs} + L_q \frac{di_{qs}}{dt} + \omega_r L_d i_{ds} + \omega_r \lambda_r \quad (5)$$

$$T_e = \frac{3}{2} p i_{qs} \lambda_r \quad (6)$$

$$T_e - T_L = J \frac{d\omega_r}{dt} + B\omega_r \quad (7)$$

where i_{ds} and i_{qs} represent the current in the dq-axis, R_s is the stator resistance, ω_r is the angular velocity, p is the number of pole pairs, λ_r is the permanent magnetic flux, T_e is the electromagnetic torque, J stands for the system inertia, B stands for the friction factor.

3 CURRENT CONTROL METHODS IN WIND TURBINE SYSTEM

In this content, two ideas are presented: first to control MPPT, second to control of MSC.

3.1 MPPT control

The MPPT technique is most commonly used with wind turbines, that is a technique used with variable power sources to maximize energy extraction as wind conditions vary. There are many MPPT methods, that have been studied and developed in industrial and academic fields [2], [3]. It includes the hill perturb and observe (P&O) algorithm, the optimal torque control (OTC), and the tip speed ratio (TSR). The TSR method uses an anemometer to estimate the wind speed, which is erratic. Errors in measurement processing, expense, and implementation complexity are some of its drawbacks [12, 13]. The output power turbine relies on the OTC's lookup table [14, 15]. An anemometer is not needed to measure wind speed when using the Perturb and Observe (P&O) approach, which is straightforward. Step size, perturbation direction, power loss, and poor efficiency, however, are the downsides [16,17]. Similarly, the saturation effect and the disturbance on the converter's input voltage are flaws in optimum controllers [18], [19]. Moreover, sliding mode control [20], nonlinear control [21] or fuzzy control [22] are frequently employed due to their high efficiency nevertheless, one of their drawbacks is that they are unable to track the maximum power point (MPP) under quickly varying conditions. Moreover, one of the difficulties is a coordinated control strategy for multiple PMSGs under rapidly changing conditions [23]. Similarly, the stable and optimal load distribution for multiple PMSGs in the grid is mentioned in [24, 25].

3.2 Control of MSCs

The following presents three d-axis current control techniques: ZDC, UPF, and CSFL.

3.2.1 ZDC

The direct-axis current i_{ds} is set to zero to make it easier to use this control mechanism ($i_{ds} = 0$). In a generator, only the quadrature-axis current i_{qs} generates torque. This control is easy to implement because of proportionality factor between torque and stator current that illustrated as Figure 2.

$$i_{ds}^* = 0 \quad (7)$$

3.2.2 UPF

In the UPF, the power factor being kept equal to one, and the stator current and stator voltage vector are in the same direction. it means

$$u_{ds}i_{qs} - u_{qs}i_{ds} = 0 \quad (8)$$

Substituting equation (4) and equation (5) into equation (8), then

$$L_s i_{ds}^2 + \lambda_r i_{ds} + L_s i_{qs}^2 = 0$$

$$\left(i_{ds} + \frac{i_m}{2}\right)^2 + i_{qs}^2 = \left(\frac{i_m}{2}\right)^2$$

This would result in a reduced size and a decrease in the cost of the power circuit and illustrated as Figure 2.

$$i_{ds}^* = \begin{cases} -\frac{i_m}{2} + \sqrt{\left(\frac{i_m}{2}\right)^2 - (i_{qs}^*)^2} & \text{Valid} \\ \frac{i_m}{2} + \sqrt{\left(\frac{i_m}{2}\right)^2 - (i_{qs}^*)^2} & \text{Not valid} \end{cases} \quad (9)$$

where $i_m = \frac{\lambda_r}{L_s}$ is the virtual current

The equation in (9) indicates that the current of the q-axis stator must be met following constraint.

$$i_{qs} \leq \frac{\lambda_r}{2L_s} \quad (10)$$

3.2.3 CSF

The stator flux vector's magnitude must be kept constant and usually set equal to rotor flux linkages.

$$|\lambda_s| = \sqrt{(L_s i_{ds} + \lambda_r)^2 + (L_s i_{qs})^2} = \lambda_r \quad (11)$$

$$\left(i_{ds} + \frac{\lambda_r}{L_s}\right)^2 + i_{qs}^2 = \left(\frac{\lambda_r}{L_s}\right)^2$$

$$(i_{ds} + i_m)^2 + i_{qs}^2 = (i_m)^2 \quad (12)$$

$$i_{ds}^* = -i_m + \sqrt{(i_m)^2 - (i_{qs}^*)^2} \quad (13)$$

A COMPARISON OF D-AXIS STATOR CURRENT...

methods, with the active power of CSF- and UPF control method are coequal ($P_{gupf} = P_{gcsf}$) that smaller than ZDC method (P_{gzdc}). Additionally, the reactive power in three control techniques are coequal ($Q_{gcsf} = Q_{gupf} = Q_{gzdc}$). According to Figure 15, the grid apparent in UPF- and CSF control method are equal value and smaller than apparent in ZDC control method. This is weaknesses of ZDC control method because of cause excess heating (losses) and undesirable voltage drops and loss of power along the transmission lines.

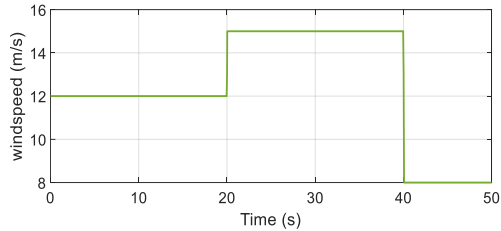


Figure 3: wind speed

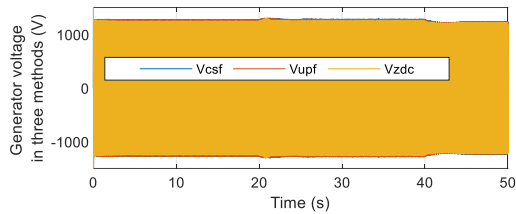


Figure 4: Generator voltage in three methods

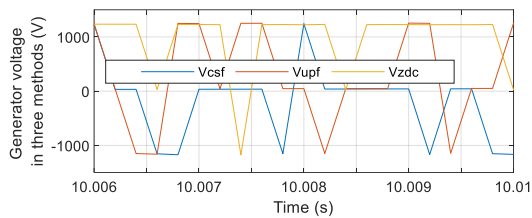


Figure 5: Zoom generator voltage in three methods

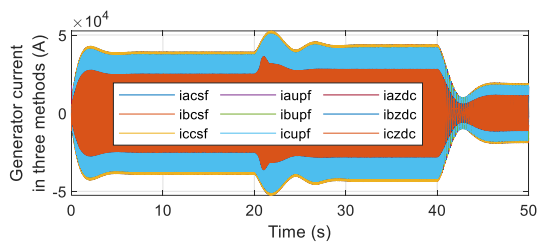


Figure 6: Generator current in three methods

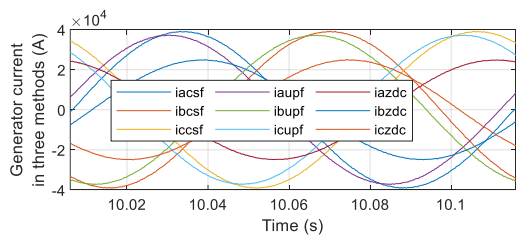


Figure 7: Zoom generator current in three methods

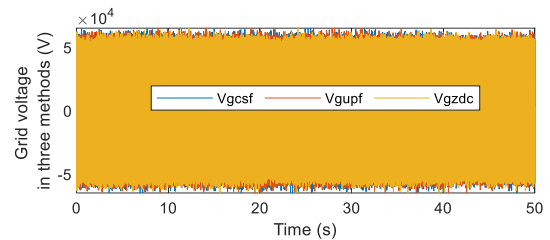


Figure 10: Grid voltage in three methods

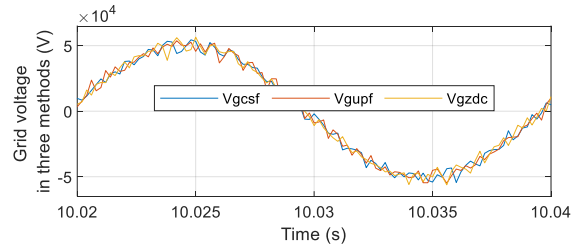


Figure 11: Zoom grid voltage in three methods

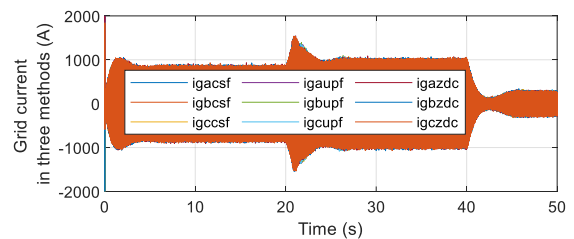


Figure 12: Grid current in three methods

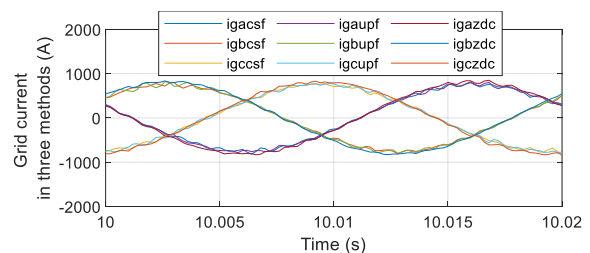


Figure 13: Zoom grid current in three methods

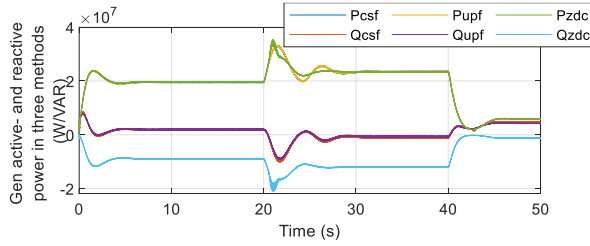


Figure 8: Generator active- and reactive power in three methods

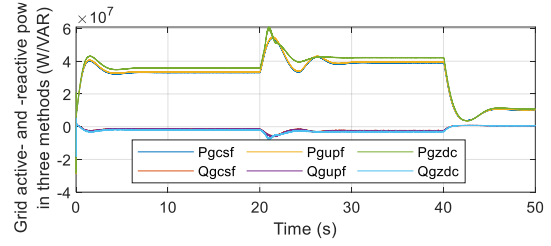


Figure 14: Grid active- and reactive power in three methods

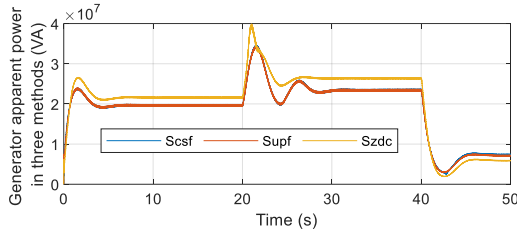


Figure 9: Generator apparent power in three methods

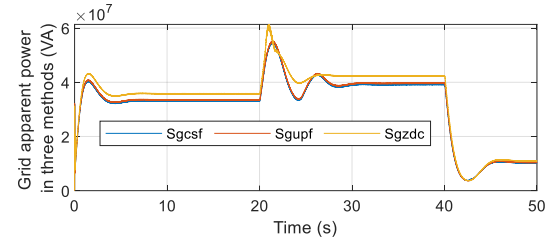


Figure 15: Grid apparent power in three methods

Table 1: Turbine parameters [2]

Symbol	Value	Descriptions
S_n	2.2 MW	Transparent power
I_n	2606 A	Nominal current
V_n	690 V	Nominal voltage
V_{dc}	1200 V	dc-link voltage
ω_n	2.355 rad/s	Nominal rotating speed
Z_p	36	Number of poles
T_e	934.2 kNm	Rated moment
B	0.004 Nms	Viscous damping
R_s	0.0008 Ω	Stator phase resistance
L_s	0.00157 H	Stator phase inductance
λ_r	9.18 Wb	Flux linkage
J	0.0000005 kg.m ²	Inertia of rotor

Table 2: PMSG parameters [2]

Symbol	Value	Descriptions
P_n	2 MW	Rated power
ω_n	2.355 rad/s	Nominal rotating speed
J	0.0000005 kg.m ²	Inertia of rotor
R	37.1 m	Blade's length

5 CONCLUSIONS

In this paper, d-axis current control methods for two PMSG operating in parallel are derived and presented in detail. Based on simulation results, our study reveals that ZDC control is superior in cost among the two different control methods because the ZDC control yields a very high reactive power, thereby big the apparent power. That is caused excess heating (losses) and undesirable voltage drops and loss of power along the transmission lines. Also, all the performance characteristics for each strategy shown above are compared. Based on our comparative study, we conclude that UPF and CSF can be considered as effective control methods, that not only attended well the maximum power but also can be reduced costly.

Future works will consider the processor-in-the-loop approach such as LAUNCHXL-F28069M for FSTPs to get reduction of the total harmonic distortion and common mode voltage in low-cost motor control and renewable energy systems.

ACKNOWLEDGMENT

This study was written by the authors under contract code: 22/2D05 and thanks to the Industrial University of Ho Chi Minh City, Vietnam for funding.

REFERENCES

- [1] Christian Breyer, Siavash Khalili, Dmitrii Bogdanov, Manish Ram, Ayobami Solomon Oyewo, Arman Aghahosseini, Ashish Gulagi, A. A. Solomon, Dominik Keiner, Gabriel Lopez, Poul Alberg Østergaard, Henrik Lund, Brian V. Mathiesen, Mark Z. Jacobson, Marta Victoria, Sven Teske, Thomas Pregger, Vasilis Fthenakis, Marco Rauegi, Hannele Holttinen, Ugo Bardi, Auke Hoekstra and Benjamin K. Sovacool, "On the History and Future of 100% Renewable Energy Systems Research," IEEE, vol. 10, pp. 78176–78218, 25 July 2022, doi: 10.1109/ACCESS.2022.3193402.
- [2] Viktor Perelmuter, "Advanced simulation of Alternative energy: Simulation with Simulink and SimPowerSystems," CRC Press, 2020.
- [3] Casper J. J. Labuschagne, and Maarten J. Kamper, "Wind Generator Impedance Matching in Small-Scale Passive Wind Energy Systems," IEEE Access, vol. 9, pp. 22558-22568, February 2021, doi: 10.1109/ACCESS.2021.3056226.
- [4] V. Yaramasu, and Bin Wu, "Model predictive control of wind energy conversion systems," Wiley-IEEE Press, 2017.
- [5] Ahmed Samir Badawi, Nurul Fadzlin Hasbullah, Siti Hajar Yusoff, Aisha Hashim, Sheraz Khan and Alhareth Mohammed Zyoud, "Paper review: maximum power point tracking for wind energy conversion system," International Conference on Electrical, Control and Instrumentation Engineering (ICECIE), November 2020, doi: 10.1109/ICECIE50279.2020.9309567.
- [6] Venkata Yaramasu, Apparao Dekka, Mario J. Durán, Samir Kouro, Bin Wu, "PMSG - based wind energy conversion systems: survey on power converters and controls," IET Electric Power Appl, vol. 11, no. 6, pp. 956–968, July 2017.
- [7] W. Xiao, "Photovoltaic Power System: Modeling, Design, and Control," United States: Wiley Press, 2017.
- [8] Hua Ye, Bo Yue, Xuan Li and Kai Strunz, "Modeling and simulation of multi - scale transients for PMSG based wind power systems," Wind Energ. vol 20, pp 1349–1364, Mar. 2017.
- [9] Zhongting Tang, Yongheng Yang and Frede Blaabjerg, "Power electronics: The enabling technology for renewable energy integration," CSEE Journal of Power and Energy Systems, vol. 8, issue: 1, pp. 39-52, January 2022, doi : 10.17775/CSEEJPES.2021.02850.
- [10] Shakir D. Ahmed, Fahad S. M. Al-Ismail, Md Shafiullah, Fahad A. Al-Sulaiman and Ibrahim M. El-Amin , "Grid Integration Challenges of Wind Energy: A Review," IEEE Access, vol. 8, pp. 10857-10878, January 2020, doi : 10.1109/ACCESS.2020.2964896.
- [11] Abdel-Raheem Youssef, Ahmed I.M. Ali, Mahmoud S.R. Saeed, Essam E.M. Mohamed. "Advanced multi-sector P&O maximum power point tracking technique for wind energy conversion system," Electrical Power and Energy Systems, vol. 107, pp. 89–97, May 2019.

- [12] Arun Kumar Maurya, Anil Kumar Rai and Hemant Ahuja, “Comparative Analysis of Different MPPT Algorithms for Roof-Top Solar PV System,” International Conference on Automation, Computing and Renewable Systems (ICACRS), February 2023, doi: 10.1109/ICACRS55517.2022.10028987.
- [13] Abdel-Raheem Youssef, Ahmed I.M. Ali, Mahmoud S.R. Saeed, Essam E.M. Mohamed, “Advanced multisector P&O maximum power point tracking technique for wind energy conversion system,” Electrical Power and Energy Systems, vol. 107, pp. 89- 97, 2019.
- [14] Hossam H.H. Mousa, Abdel-Raheem Youssef, I. Hamdan, Maqusood Ahamed and Essam E.M. Mohamed, “Variable step size P&O MPPT algorithm for optimal power extraction of multi-phase PMSG based wind generation system,” Electrical Power and Energy Systems, vol. 108, pp. 218–231, 2019.
- [15] Mekalathur B. Hemanth Kumar, Balasubramanian Saravanan, Padmanaban Sanjeevikumar and Frede Blaabjerg, “Review on control techniques and methodologies for maximum power extraction from wind energy systems,” IET Renewable Power Generation, September 2018.
- [16] Hossam H.H. Mousa, Abdel-Raheem Youssef, I. Hamdan, Maqusood Ahamed and Essam E.M. Mohamed, “Performance Assessment of Robust P&O Algorithm Using Optimal Hypothetical Position of Generator Speed,” IEEE, vol. 9, 2021.
- [17] Adeyemi Taylor and Sarhan M. Musa, “Evaluation of Hybrid AI-based Techniques for MPPT Optimization,” International Conference on Green Energy, Computing and Sustainable Technology (GECOST), October 2022, doi: 10.1109/GECOST55694.2022.10010563.
- [18] F. Bakhtiari and J. Nazarzadeh, “Optimal Estimation and Tracking Control for Variable-speed Wind Turbine with PMSG,” Journal of Modern Power Systems and Clean Energy, vol. 8, no. 1, pp. 159-167, January 2020, doi: 10.35833/MPCE.2018.000365.
- [19] H. H. H. Mousa, A. R. Youssef, E. E. M. Mohamed, “Optimal power extraction control schemes for five-phase PMSG based wind generation systems,” Engineering Science and Technology an International Journal, vol. 23, no. 1, pp 144-155, 2020, doi: 10.1016/j.jestch.2019.04.004.
- [20] N. Z. Laabidine, A. Errarhout, C. E. Bakkali, K. Mohammed, B. Bossoufi, “Sliding mode control design of wind power generation system based on permanent magnet synchronous generator,” International Journal of Power Electronics and Drive System (IJPEDS), vol. 12, no. 1, pp. 393-403, 2021, doi: 10.11591/ijpeds.v12.i1.pp393-403.
- [21] K. Noussi, A. Abouloifa, H. Katir, I. Lachkar, and F. Giri, “Nonlinear control of grid-connected wind energy conversion system without mechanical variables measurements,” International Journal of Power Electronics and Drive System (IJPEDS), vol. 12, no. 2, pp. 1139-1149, 2021, doi: 10.11591/ijpeds.v12.i2.pp1139-1149.
- [22] R. Subramaniam and Y. H. Joo, “Passivity-Based Fuzzy ISMC for Wind Energy Conversion Systems With PMSG,” IEEE Transactions on Systems, Man, and Cybernetics: Systems, vol. 51, no. 4, pp. 2212-2220, 2021, doi: 10.1109/TSMC.2019.2930743.
- [23] Yanjian Peng, Yong Li, Kwang Y. Lee, Yi Tan, Yijia Cao, Ming Wen, Yangwu Shen, Mingmin Zhang and Wenguo Li, “Coordinated Control Strategy of PMSG and Cascaded H-Bridge STATCOM in Dispersed Wind Farm for Suppressing Unbalanced Grid Voltage,” IEEE Transactions on Sustainable Energy, vol. 12, issue. 1, pp. 349-359, 2021, doi: 10.1109/TSTE.2020.2995457.
- [24] Peng Kou, Deliang Liang, Lin Gao, “Distributed Coordination of Multiple PMSGs in an Islanded DC Microgrid for Load Sharing,” IEEE Transactions on Energy Conversion, vol. 32, issue. 2, pp. 471-485, 2017, doi: 10.1109/TEC.2017.2649526.
- [25] Peng Kou, Deliang Liang, Junmin Wang, Lin Gao, “Stable and Optimal Load Sharing of Multiple PMSGs in an Islanded DC Microgrid,” IEEE Transactions on Energy Conversion, vol. 33, issue. 1, pp. 260-271, 2018, doi: 10.1109/TEC.2017.2755461.

SO SÁNH CÁC PHƯƠNG PHÁP ĐIỀU KHIỂN DÒNG STATOR TRỤC D CHO HAI MÁY PHÁT ĐIỆN PMSG VẬN HÀNH SONG SONG TRONG HỆ THỐNG TURBINE GIÓ

NGUYEN NGOC ANH TUAN ^{1*}, DUY CONG PHAM ¹, NGUYEN THANH THAO ¹,
VO THI ANH TUYET ¹, BUI HONG PHONG ²

¹ Khoa Điện, Trường Đại học Công nghiệp Thành phố Hồ Chí Minh

² Trường Cao Đẳng Kinh tế và Kỹ thuật Nguyễn Hữu Cảnh

*Tác giả liên hệ: nguyennngocanh tuan@iuh.edu.vn

Tóm tắt. Bài báo đề xuất nghiên cứu kỹ thuật điều khiển dòng stator trục d cho bộ biến đổi phía máy trong máy phát điện đồng bộ nam châm vĩnh cửu dựa trên hai hệ thống tuabin gió hoạt động song được nối vào lưới điện thông qua bộ biến đổi ngược chiều. Phần trình bày ngắn gọn về các kỹ thuật điều khiển dòng điện stator có trục d. Trước hết là kỹ thuật điều khiển dòng stator trục d bằng 0 (ZDC), tiếp theo là kỹ thuật điều khiển hệ số công suất đồng nhất (UPF) và thứ ba là kỹ thuật điều khiển liên kết từ thông stator không đổi (CSF). Các nghiên cứu so sánh được trình bày để xác nhận các tính năng thuận lợi của các phương pháp được đề xuất. Hiệu quả của đề xuất được đánh giá và so sánh thông qua kết quả mô phỏng dựa trên MATLAB. Kết quả so sánh cho thấy tính ưu việt của phương pháp đề xuất được chứng minh bằng việc điều khiển dòng stator trục d không những có thể đạt được công suất cực đại mà còn có thể giảm chi phí.

Từ khóa. Máy phát điện đồng bộ nam châm vĩnh cửu, điều khiển dòng điện stator trục d bằng không, điều khiển hệ số công suất không đổi, điều khiển từ thông stator không đổi.

Ngày nhận bài: 16/9/2023

Ngày chấp nhận đăng: 11/4/2024